JOURNAL OF ENGINEERING SCIENCES

Volume 8, Issue 1 (2021)

Nogueira E. (2020). Applying the concepts of efficiency and effectiveness to analyze the influence of the number of passes in the shell and tubes condenser thermal performance. Journal of Engineering Sciences, Vol. 8(1), pp. F1–F10, doi: 10.21272/jes.2021.8(1).f1

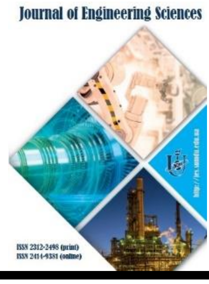

Applying the Concepts of Efficiency and Effectiveness to Analyze the Influence of the Number of Passes in the Shell and Tubes Condenser Thermal Performance

Nogueira E.

Department of Mechanics and Energy, State University of Rio de Janeiro,
R. São Francisco Xavier, 524 Maracanã, Rio de Janeiro, 20550-013 Brazil

Article info:
Received: December 9, 2020
The final version received: April 24, 2021
Accepted for publication: May 1, 2021

***Corresponding email:**
elcionogueira@hotmail.com

Abstract. The work analyzes the influence of the number of passes in a shell and tubes condenser heat exchanger, with an inlet pressure of R134a refrigerant in the shell equal to 1.2 MPa. The fluid that circulates in the tubes is water or water-based nanofluid with a fraction of aluminum oxide nanoparticles (Al_2O_3), and the methodology used subdivides the heat exchanger into three distinct regions: the overheated region, the saturated region, and the subcooled region. The main parameters used to analyze the thermal performance of the heat exchanger were efficiency and effectiveness. Efficiency in the superheated steam region is close to 1.0. There is scope for increasing thermal effectiveness, which can be improved with more significant passes in the tube. The saturated steam region process is efficient for lower mass flow rates of the fluid in the tube, but it is ineffective. However, it is highly effective for high mass flow rates. There is ample scope for increasing effectiveness in the subcooled region. Still, the fluid inlet temperature in the pipe and the work refrigerant pressure are the limiting factors for greater heat exchange in the subcooled region.

Keywords: heat exchange, refrigerant, tube condenser, thermal performance.

1 Introduction

The article aims to analyze the influence of the number of passes on the tube in a shell and tubes condenser heat exchanger using the concepts of efficiency and effectiveness.

The heat exchanger used as a base consists of a shell and 36 tubes, with three regions of 12 tubes each. The refrigerant is R134a, and the nanofluid in the tubes is based on water and a fraction of aluminum oxide nanoparticles (Al_2O_3). The refrigerant's working pressure is equal to 1.2 MPa, and the inlet temperature is equal to 70.5 °C. The fluid flowing in the tubes has an inlet temperature equal to 25 ºC. The shell and tube condenser heat changer in question was analyzed experimentally and theoretically by Lee and Mai [1], and theoretically by Nogueira [2].

2 Literature Review

One of the essential components in a heat pump is the condenser, which transfers energy from the refrigerant to water or another fluid at a lower temperature. Shell and tube condensers are the most commonly used for heating water for their adaptability and easy construction. Heat pumps are considered moderately high temperatures when the fluid's outlet temperature to be heated varies from 60 °C to 95 °C. In these operating conditions, the temperature difference between inlet and outlet may be above 40 °C, and that the condensation temperature increases, resulting in a decrease in thermal efficiency. The factors that can influence the thermal performance in the shell and tube condenser are many and deserve in-depth investigation in all aspects [1].

The methodology [2] uses the concepts of efficiency and effectiveness to analyze the thermal performance of a shell and tube condenser, with Freon 134a as a refrigerant flowing in the shell at relatively low saturation pressure. Water or water-based aluminum oxide nanoparticles flow in the tubes. The condenser is divided into three regions to facilitate analysis, with four pipes and three passes: 12 tubes. The refrigerant mass flow rate is fixed equal to 0.20 kg/s. As a basis for obtaining theoretical results, the experimental result obtained from reference [1] was used, with a vapor pressure value equal to 1.2 MPa and a water flow equal to 0.41 kg/s.

Bejan [3] presented a procedure to minimize entropy generation at a physical system's components. The work's fundamental idea is to demonstrate that the system's entropy generation rate is the sum of the contributions of all components. If the irreversibility of a component is minimized, the reduction occurs at the system's general level.

Fakheri [4] presented a solution for defining thermal efficiency in heat exchangers applying thermodynamics' second law. It demonstrates that there is an ideal heat exchanger for each real heat exchanger that has the same thermal resistance, the average temperature difference, and the same temperature ratio of cold to the hot fluid inlet. The ideal heat exchanger transfers maximum energy and generates a minimum amount of entropy, making it more efficient and less irreversible. The article provides a new way to analyze heat exchangers and heat exchanger networks.

Tiwari and Maheshwari [5] demonstrated that a heat exchanger's better thermal performance results from efficient energy use and allows for weight reduction. They claim that a heat exchanger's performance is generally measured by its effectiveness, which does not provide any information about its efficiency. The concept of thermal efficiency must be based on the second law of thermodynamics. Through this procedure, the relationship between effectiveness and efficiency can be explained mathematically.

Hermes [6] presented an approach for the optimum design of condensers and evaporators. He put forward an explicit formulation that expresses the dimensionless rate of entropy generation and an expression for the optimum heat exchanger effectiveness, based on the working conditions, heat exchanger geometry, and fluid. It was found that a heat exchanger design with a high aspect ratio is preferable to a low aspect ratio, and the heat exchanger design that presents the best component-level also leads to the best global system performance.

Nogueira [7, 8] presented an analytical solution for obtaining the outlet temperatures in a shell and tube heat exchanger. He uses the concepts of efficiency, effectiveness (ε-NTU), and irreversibility. The nanoparticles' volume fractions ranging from 0.1 to 0.5, and the results for efficiency, effectiveness, and irreversibility were obtained graphically. The flow laminarization effect for nanofluid particles had significant relevance in the results.

The chemical characteristics of refrigerants alternative to CFCs have been proposed and implemented by the refrigeration industries. HFC-134a is one of the options found to replace CFC-12 due to similar physical properties. The change in refrigerant in refrigeration equipment has led to a detailed investigation of the properties of HFC-134a [9].

The refrigerant R134a is considered a suitable alternative for reducing the effect of refrigerants on the ozone layer. The work presented by Roy and Mandal [10] uses liquid density, saturation vapor pressure, state equation, and specific heat at constant volume to obtain mathematical expressions, equations to determine different thermodynamic properties of the refrigerant R-134a. These equations and Maxwell's relations make it possible to calculate enthalpy and entropy for the vapor state.

The condensation process of R134a refrigerant in the circular and flat tubes was investigated numerically by Wen et al. [11]. Two correlations were developed and compared with existing correlations that underestimate both the heat transfer coefficients and pressure gradients.

A circular tube and three-flat copper tubes were used to determine the aspects associated with the condensation enthalpy of R134a. The experimental results demonstrated that the existing correlations are not appropriately applied for the flattened pipes. A new correlation was developed by Kaew-On et al. [12], based on the experimental data.

Albadr et al. [13] reported an experimental study on heat transfer and nanofluid flow with different concentrations in a volume of aluminum oxide – Al_2O_3 (0.3–2.0 %) in a shell and tube heat exchanger under turbulent conditions. The convective heat transfer coefficient results demonstrate that the nanofluid has a thermal performance slightly superior to that of water at the same mass flow and inlet temperature. However, the increase in the concentration of nanoparticles causes an increase in the friction factor.

Heat exchangers are used in many applications, such as air conditioning and domestic water heating. The work developed by Almurtaji et al. [14] provides a systematic review of the use of nanofluids to improve the thermo-hydraulic of such equipment. The objective is to emphasize the importance of nanofluids and how their use significantly increases heat exchangers' thermal efficiency.

3 Research Methodology

3.1 General formulation

Figure 1 shows a diagram for the condenser under analysis. The condenser was divided into three regions. The regions consist of 12 pipes each: 4 tubes in line and three passages in each region. The steam enters the overheated region at a temperature equal to 70.5 °C. The fluid enters at a temperature equal to 25 °C in the subcooled region. There are three horizontal baffles in the supersaturated steam region to increase the efficiency of heat exchange. The steam flow is equal to 0.20 kg/s. The flow rate of the fluid in the tube varies from 0.05 kg/s to 0.40 kg/s. The properties of fluids are shown in Table 1.

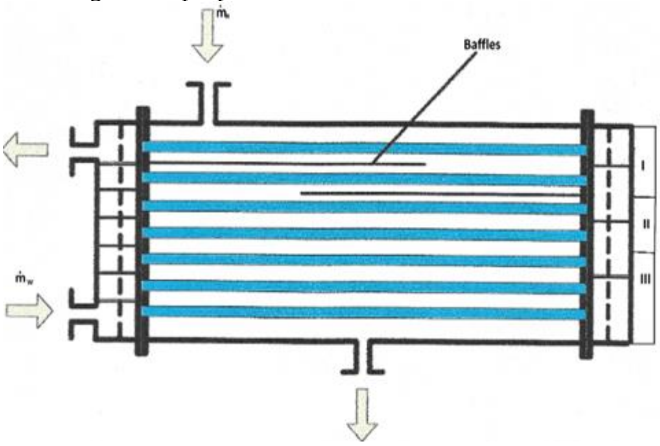

Figure 1 – Scheme for the shell and tubes condenser

Table 1 – Properties of the fluids and nanoparticle

Properties	Freon R134a		Water	Al_2O_3
	I	III		
k, W/(m K)	15.4	74.71	0.60	31.9
Cp, J/(kg K)	1,144	1,498	4180	837
μ, 10^{-6} kg/(m s)	12.3	161.45	75.8	4.65
ρ, kg/m^3	50	1,146	997	3950
ν, 10^{-7} N·m^2/s	2.47	1.40	0.80	0.118
α, 10^{-6} m^2/s	269.0	43.5	0.143	9.65
Pr	1,091	310.7	5.68	818

The initial input data, three passes, for each of the regions are: TREntr = 70.5 ºC; TWEntr = 25.0 ºC; Tsat = 46.02 ºC;

$$NTube = 4; \tag{1}$$

$$Npass = 3; \tag{2}$$

$$D_W = 0.0127\, m; \tag{3}$$

$$L = 0.762\, m; \tag{4}$$

$$B = 0.0145\, m; \tag{5}$$

$$CL = 1.0; \tag{6}$$

$$CTP = 0.85. \tag{7}$$

So, we have:

$$Pt = 1.25 D_W; \tag{8}$$

$$De = \frac{1.27}{DW}(Pt^2 - 0.785 DW^2); \tag{9}$$

$$Dc = 3.0 D_W; \tag{10}$$

$$PR = \frac{Pt}{DW}; \tag{11}$$

$$A_W = \pi D_W L NtubeNpass; \tag{12}$$

$$Ds = 0.637\sqrt{CL/CTP}\sqrt{ATPR^2 Dc/L}; \tag{13}$$

$$As = DsB\left(1.0 - \frac{DW}{Pt}\right); \tag{14}$$

Pt is the tube pitch, DW is the tube diameter, De is the equivalent hydraulic diameter, B is the baffles spacing, Ds is the shell diameter associated with each Region, AW is the heat exchange area, As is the shell-side pass area.

$$Re_R = \frac{\dot{m}_R De}{As\, \mu_R}; \tag{15}$$

$$Nu_R = 0.36 {Re_R}^{0.55} {Pr_R}^{1/3}. \tag{16}$$

At where, $\dot{m}_R$ is the mass flow, μ_R is the dynamic viscosity of the refrigerant, Re_R is the Reynolds number, Pr_R is the Prandtl number and Nu_R is the Nusselt number.

$$h_R = \frac{Nu_R\, k_R}{De}, \tag{17}$$

where k_R is the thermal conductivity and h_R is the convection heat transfer coefficient;

$$\rho_W = \phi\rho_{Al} + (1-\phi)\rho_W; \tag{18}$$

$$\mu_W = (1 + 2.5\phi)\mu_W; \tag{19}$$

$$\nu_W = \frac{\mu_W}{\rho_W}; \tag{20}$$

$$Cp_W = [\phi\rho_{Al}Cp_{Al} + (1-\phi)\rho_W Cp_W]/\rho_W; \tag{21}$$

$$k_W = \frac{K_{Al} + 2k_W + 2(k_{Al} - k_W)(1+0.1)^3\phi}{(K_{Al} + 2k_W - (k_{Al} - k_W)(1+0.1)^2\phi)} k_W; \tag{22}$$

$$\alpha_W = \frac{k_W}{\rho_W Cp_W}; \tag{23}$$

$$Pr_W = \frac{\alpha_W}{\nu_W}, \tag{24}$$

where ρ_W is the density of the flud, μ_W is the dynamic viscosity of the fluid, ν_W is the kinematic viscosity of the fluid, Cp_W is the specific heat of the fluid, k_W is the thermal conductivity and Pr_W is Prandtl number.

$$\dot{m}_{WT} = \dot{m}_W / N_{Tube}; \tag{25}$$

$$Re_W = \frac{4\dot{m}_{WT}}{\pi D_W\, \mu_W}, \tag{26}$$

where $\dot{m}_W$ is the flow inlet of the fluid, $\dot{m}_{WT}$ is the flow in each tube and Re_W is the Reynolds number;

$$Nu_W = 4.364 + \frac{0.0722 Re_W\, Pr_W\, D_W}{L}$$
$$for\ Re_W \le 2{,}100; \tag{27}$$

$$Nu_W = \frac{\left[\left(\frac{ft}{8}\right)(Re_W - 10^3)Pr_W\right]\left(1 + \frac{D_W}{L}\right)^{0.67}}{1 + 1.27\sqrt{\frac{ft}{8}}\left({Pr_W}^{0.67} - 1\right)}$$
$$for\ 2{,}100 < Re_W \le 10^4; \tag{28}$$

$$ft = [1.82 Log(Re_W) - 1.64]^{-2}; \tag{29}$$

$$Nu_w = 0.027 {Re_w}^{0.8} {Pr_w}^{1/3}\ for\ Re_W > 10^4; \tag{30}$$

ft is the friction factor and Nu_W is the Nusselt number.

$$h_W = (Nu_W\, K_W)/D_W; \tag{31}$$

$$Uo = \frac{1}{\frac{1}{h_R} + \frac{1}{h_W}}, \tag{32}$$

where U_O is the global heat transfer coefficient;

$$C_R = \dot{m}_R Cp_R; \tag{33}$$

$$C_W = \dot{m}_W Cp_W; \tag{34}$$

$$NTU = \frac{A_W\, U_O}{Cmin}; \tag{35}$$

$$Fa = (NTU/2)(1 - C_*); \tag{36}$$

$$C_* = Cmin/Cmax; \tag{37}$$

C_R is the thermal capacity of the refrigerant, C_W is the thermal capacity, NTU is called the Number of Thermal Units, Cmin is the smallest of the specific heats;

$$\sigma_T = tanh(Fa)/Fa; \tag{38}$$

$$\eta_T = \frac{1}{\frac{1}{\sigma_T\, NTU} + \frac{1 + C_*}{2}}; \tag{39}$$

σ_T is thermal efficiency and η_T is the thermal effectiveness.

3.2 Solution procedure for the region I

$$TW_i = T_{sat} - \Delta T_1, \quad (40)$$

where ΔT_1 – the actual temperature of the fluid inlet in Region I for a given flow in the tube. The experimental data from reference [1] (Table 1) were used: inlet temperature equal to 70.5 °C, and mass flow for the tube fluid equal to 0.41 kg/s. Then, we define:

$$\Delta T_1 = 0.0\ for\ theoretical\ results; \quad (41)$$
$$\Delta T_1 = 2.0\ for\ experimental\ results; \quad (42)$$
$$TR_i = TREntr; \quad (43)$$
$$Q_{Actual} = \frac{(TR_i - TW_i)Cmin}{\frac{1}{\sigma_T\ NTU} + \frac{1 + C_*}{2}}; \quad (44)$$
$$TW = (Q_{actual}/C_W) + TW_i; \quad (45)$$
$$TR = TR_i - (Q_{Actual}/C_R), \quad (46)$$

where Q_{Actual} – the heat exchange between fluids, TW_i is the fluid inlet temperature, TR_i is the fluid inlet temperature.

Then,

$$TR_i = TR_i - \epsilon_1. \quad (47)$$

Return to equation (44) and recalculate Q_{Actual}, TW, and TR.

ϵ_1 It is a value that allows precision in determining TR and TW.

The procedure at Region I ends when:

$$TR_i \leq Tsat. \quad (48)$$

3.3 Solution procedure for the region II

$$X = 1; \quad (49)$$
$$hlv = hv - hl; \quad (50)$$
$$\mu_R = \mu_{Rl}X + \mu_{RV}(1 - X); \quad (51)$$
$$\rho_R = \rho_{Rl}X + \rho_{RV}(-X); \quad (52)$$
$$k_R = k_{Rl}X + k_{RV}(1 - X); \quad (53)$$
$$Cp_R = Cp_{RL}X + Cp_{RV}(1 - X); \quad (54)$$
$$Pr_R = Pr_{Rl}X + Pr_{RV}(1 - X), \quad (55)$$

where X – the steam fraction in Region II;

$$Re_R = (\dot{m}_R De)/(As\ \mu_R); \quad (56)$$
$$\Delta_f = Tsat - T_{REf}; \quad (57)$$
$$h_R = 0.943\left[k_R \rho_R\ ghlv/(\mu_R Ds \Delta_f)\right]^{0.25}, \quad (58)$$

where Re_R – the number of Reynolds in Region II; Δf – a reference temperature difference; h_R is the convection heat transfer coefficient, and $T_{REf} = 0$.

h_R varies with properties. The heat exchange between fluids in Region II is achieved by:

$$\sigma_T = \frac{tanh(Fa)}{Fa}; \quad (59)$$
$$\eta_T = \left(\frac{1}{\sigma_T\ NTU} + \frac{1 + C_*}{2}\right)^{-1}; \quad (60)$$
$$Q_{Actual} = \frac{(Tsat - TW_i)Cmin}{\frac{1}{\sigma_T NTU} + \frac{1 + C_*}{2}}; \quad (61)$$
$$TW = TW_i - (Q_R/C_*); \quad (62)$$

Therefore:

$$TW_i = TW_i - \epsilon_2 \quad (63)$$

Return to Equation 60 and recalculate Q_{Actual}, TW.

ϵ_2 It is a value that allows precision in determining *TW*.

The procedure at Region II ends when:

$$X < 0. \quad (64)$$

3.4 Solution procedure for the region III

$$TW_i = 25\ °C; \quad (65)$$
$$TR_i = Tsat. \quad (66)$$

The initial calculations use the properties as shown in Table 1, Region III. Then equations 15 to 17, 33 to 39 must be recalculated.

$$Q_{Actual} = \frac{(TR_i - TW_i)Cmin}{\frac{1}{\sigma_T\ NTU} + \frac{1 + C_*}{2}}; \quad (67)$$
$$TW_o = TW - (Q_{Actual}/C_W); \quad (68)$$
$$TR_o = TR - (Q_{Actual}/C_R); \quad (69)$$
$$\mathrm{TW} = TW_o; \quad (70)$$
$$TR = TR - \Delta T_2. \quad (71)$$

Therefore,

$$TW_i = TW_i - \epsilon_2. \quad (72)$$

Return to equation (67) and recalculate Q_{Actual}, TWo, and TRo.

ϵ_2 It is a value that allows precision in determining *TRo* and *TWo*.

The procedure at Region III ends when:

$$TW_i \leq TWEntr. \quad (73)$$

In this case, we have the outlet temperature of the refrigerant.

ΔT_2 allows determining the real temperature of the fluid inlet in Region I. The experimental data of Table 1 of the reference [1] is used as reference: Inlet temperature equal to 70.5 °C, refrigerant pressure equal to 1.2 MPa, and mass flow equal to 0.41 kg/s. Then, we define:

$$\Delta T_2 = 0\ for\ theoretical\ results; \quad (74)$$
$$\Delta T_2 = 0.085\ for\ the\ experimental\ results. \quad (75)$$

4 Results and Discussion

4.1 Region I – superheated steam

In the region of superheated steam of the heat exchanger in question, Region I, already described and represented by Figure 1, there are three well-defined temperatures: fluid inlet temperature in the tubes, refrigerant inlet temperature R134a, and pressure saturation temperature equal to 1.2 MPa, that is, 46.02 °C. The energy available for heat exchange depends on the temperatures of the refrigerant. With an inlet temperature equal to the outlet temperature of Region II, the fluid entering the tubes of saturated steam absorbs all the energy, and its outlet temperature depends on its mass flow rate. Less mass flow rate, higher outlet temperature, due to its lower thermal capacity; that is, there is a more significant temperature variation per unit mass. As the nanofluid has thermal diffusivity higher than that of water, its outlet temperature is slightly higher.

Figure 2 presents results for temperature profiles for nanofluid in Region I, superheated steam, for two lengths of the heat exchanger, L_1 = 0.762 m and L_2 = 1.016 m, and three different flow rates for the flow of the fluid in the tube, 0.05 kg/s, 0.20 kg/s, and 0.40 kg/s. There is a proportional increase of 33.33% in the heat exchanger's length, which provided a maximum increase in the fluid's outlet temperature in the tube equal to 4.3 %, for the lowest flow rate, equal to 0.05 kg/s. The increase in the outlet temperature is insignificant for higher flow rates due to the greater thermal capacity. Increasing the heat exchange area through a longer heat exchanger length is not advantageous when higher outlet temperatures are desired for the tubes' fluid since this procedure is economically more expensive.

Figure 3 presents results for temperature profiles in Region I for water and nanofluid (Al_2O_3). The flow of the fluid in the tube is equal to 0.050 kg/s, that is, the flow that allows the highest outlet temperature in the analysis in question. The number of passes in the tube varies from 3 to 6 passes; that is, the heat exchange area is doubled. The outlet temperature observed between these extremes increases by 6.85 % for the nanofluid and 6.22 % for water. Since it is undoubtedly a less costly procedure than doubling the heat exchanger's length, Auspicious results affect not only Region I but also other regions.

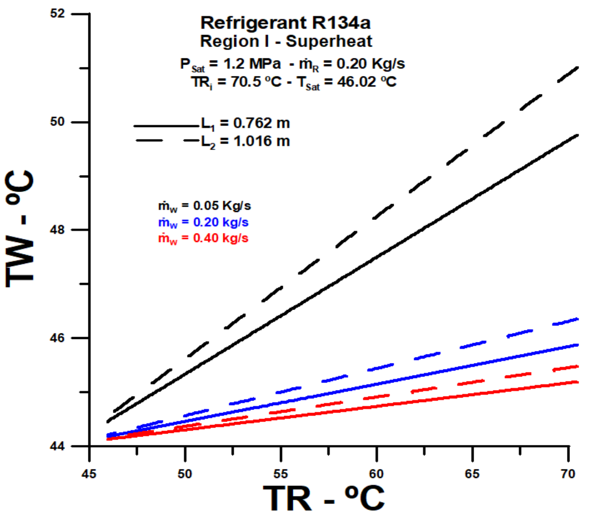

Figure 2 – Influence of heat exchanger length and fluid flow in the tube

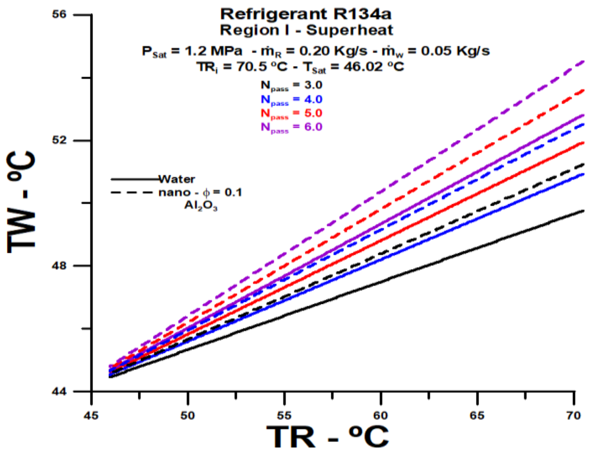

Figure 3 – Influence of the number of passes on the tube on the temperature profile in Region I

The fluid outlet temperature in the tubes in Region I, as a function of the mass flow rate, is represented by Figure 4, for water and nanofluid. As previously noted, the highest outlet temperature corresponds to the lowest flow in the analysis. However, as the tubes' flow increases, the difference between the outlet temperatures, when the number of passes in the tube is doubled, decreases progressively as the flow rate varies from laminar to turbulent regime. It is not advantageous to increase the number of passes for flow rates above 0.3 kg/s, for Reynolds number above 10^4, within the range of flow rates analyzed, when what is desired is the highest possible outlet temperature for the fluid in the tubes.

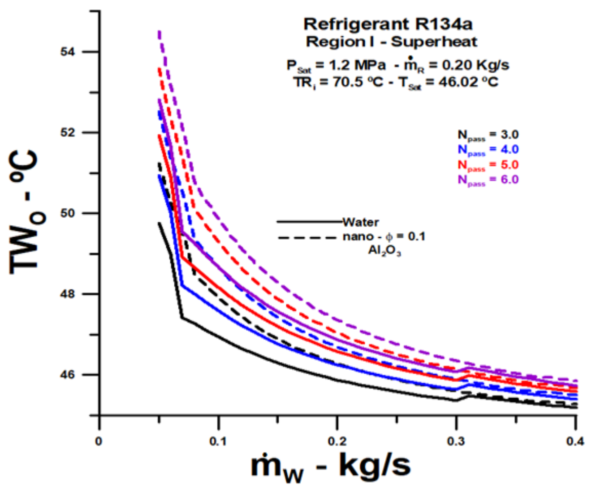

Figure 4 – Influence of the number of passes in the tube on the outlet temperature in Region I

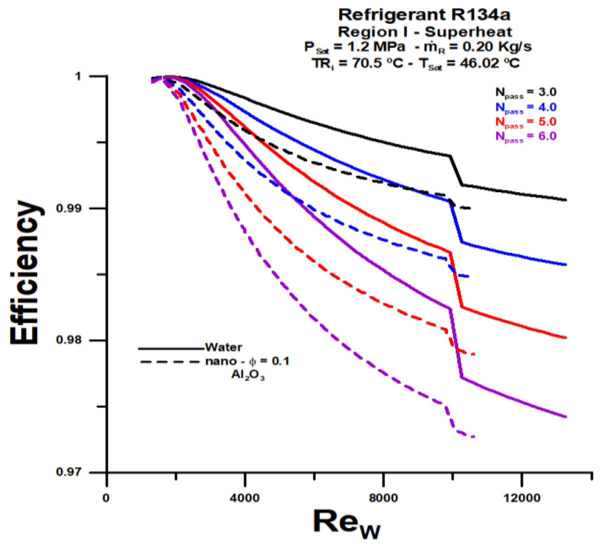

Figure 5 - Influence of the number of passes on the tube on thermal efficiency in Region I

Thermal efficiency in Region I is represented by Figure 5, using the number of passes in the tube as a parameter. Efficiency is exceptionally high in all situations analyzed. However, there is a slight decrease when the number of passes increases and when the flow regime varies from laminar to turbulent. For lower flow, equal to 0.05 kg/s, the efficiency is equal to 1 regardless of the number of passes. This result reflects the fact that there is a more significant temperature variation between inlet and outlet in this flow rate.

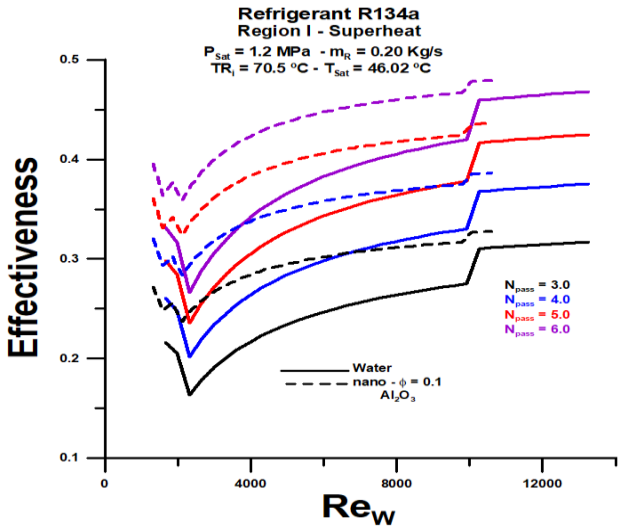

Figure 6 – Influence of the number of passes on the tube on the thermal effectiveness in Region I

Thermal effectiveness in Region I is represented by Figure 6, using the number of passes in the tube as a parameter. The effectiveness is doubled practically when the number of passages in the pipe is doubled for the entire flow range analyzed, varying from 0.2 to 0.4 for flow equal to 0.05 kg/s. Despite this, effectiveness is relatively low, demonstrating that not all of the potential for heat exchange is tapped; that is, the heat exchange is below the maximum possible for the number of passes under analysis.

As a summary for Region I:

1) we can say that the mass flow rate that allows the highest outlet temperature is the lowest possible, equal to 0.05 kg/s;

2) the outlet temperature increases as the number of passes through the tube increases;

3) there is scope for increasing thermal effectiveness, although efficiency is very close to 1 in all cases;

4) the effectiveness can be improved with a more significant number of passes in the tube;

5) the heat exchange process in Region I is efficient, it works, but it can become more effective when it comes to obtaining the highest possible outlet temperature for the fluid in the tube.

4.2 Region II – saturated steam

In the region of saturated steam of the heat exchanger in question, Region II, already described and represented through Figure 1, there are two well-defined temperatures: fluid outlet temperature in the tubes and the saturation temperature in the pressure equal to 1.2 MPa, that is, 46.0 °C. However, the quantity of relevant importance is the enthalpy available for each steam fraction X, which varies between dry saturated steam, $X = 1$, and subcooled liquid, $X = 0$. The available energy, therefore, depends on the enthalpy available between these two extremes. As the refrigerant's mass flow rate is constant, equal to 0.20 kg/s, the available energy is the same for all liquid flows in the tubes.

The fluid that passes through the tubes enters Region II with an unknown temperature, to be determined using the methodology described above.

The fluid temperature in the tubes entering Region I and leaving Region II depends on the number of passes in the tube, as shown in Figure 7 below. Although close, there is a slight difference between the number of passes, and a smaller number of passes has a lower outlet temperature in Region II, as shown in Figure 3. As the mass flow rate of the fluid in the tubes is the same, equal to 0.05 kg/s, a more extensive exchange area, that is, a more significant number of passes in the tube absorbs a greater amount of energy, which reflects a more substantial difference in temperature between the entrance and the exit of Region II.

Figure 8 shows the inlet temperatures in Region II to function the number of passes in the tube and the fluid's mass flow rate. As discussed in the paragraph above, in Figure 7, the highest inlet temperature in Region II corresponds to the lowest number of passes in the tube, equal to three passes.

Thermal efficiency in Region II is represented by Figure 9, using as a parameter the number of passes in the tube. Efficiency is equal to 1.0 for lower flow rate, equal to 0.05 kg/s, regardless of the number of passes, and falls progressively as the flow rate increases, with significant dependence on the number of passes. The efficiency is 0.6 for water and 0.5 for nanofluid when the number of passes is equal to 6, and the tubes' flow corresponds to 0.40 kg/s.

The thermal effectiveness in Region II is represented by Figure 10, using the number of passages in the tube, and varying the pipes' flow. The effectiveness increases progressively with the mass flow rate variation, varying between 0.4, for mass flow rate equal to 0.05 kg/s, to 0.8, for mass flow rate equal to 0.40 kg/s, when the number of passes is equal to 3.

When the number of passes in the tube is 6, the effectiveness approaches 1.0 for the highest mass flow rate in the pipes: 0.40 kg/s. Therefore, in this situation, the heat exchange comes at the maximum possible in Region II.

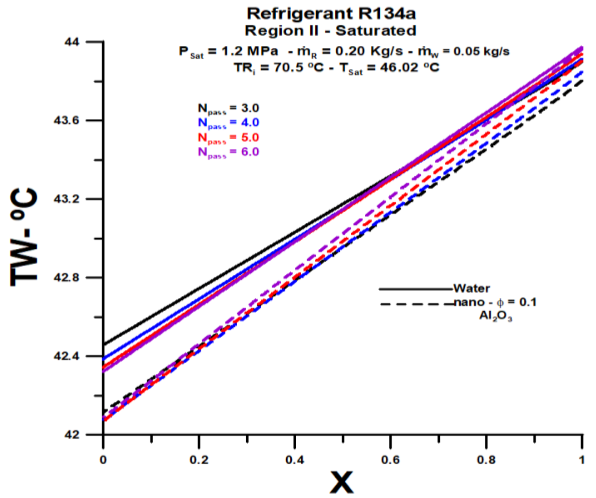

Figure 7 – Influence of the number of passes on the tube on the temperature profile in Region II

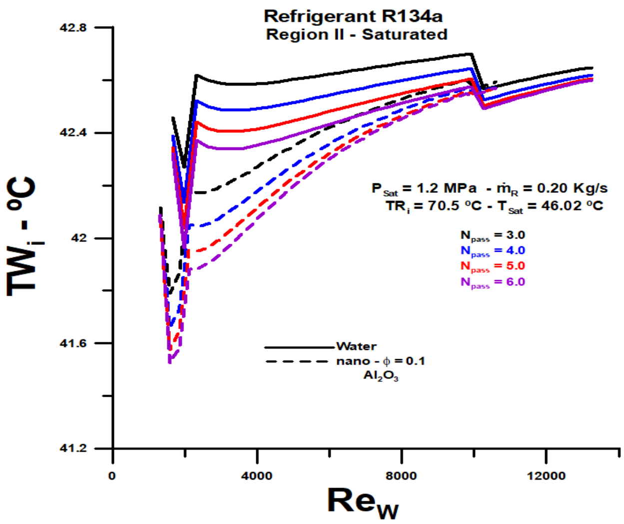

Figure 8 – Influence of the number of passes on the temperature of entry in Region II

In summary, for Region II:

1) the highest inlet temperature is obtained for the lowest flow in the pipe and the lowest number of passes;

2) efficiency is high, close to 1.0, regardless of the number of passes in the tube;

3) the effectiveness is low for lower flows, and the number of passes equal to 3;

4) the effectiveness is rising to values close to 0.8 for a higher flow rate: 0.40 kg/s.

Region II's heat exchange process is efficient, works for lower mass flow rates of the fluid in the tube and fewer passes in the pipe. However, it is not effective; that is, it does not absorb all the available energy.

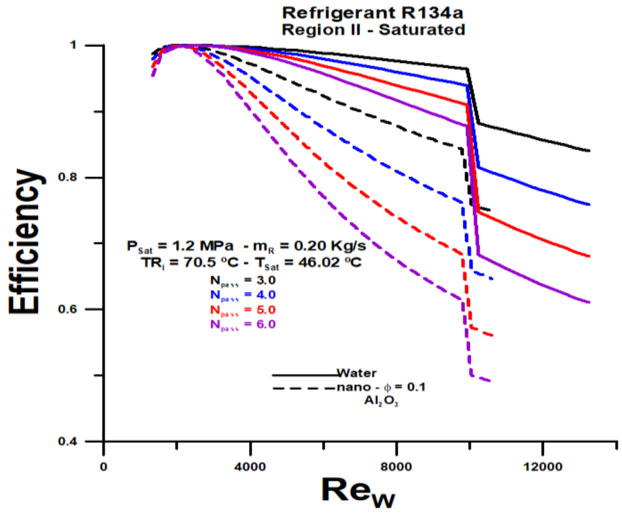

Figure 9 – Influence of the number of passes on the tube on thermal efficiency in Region II

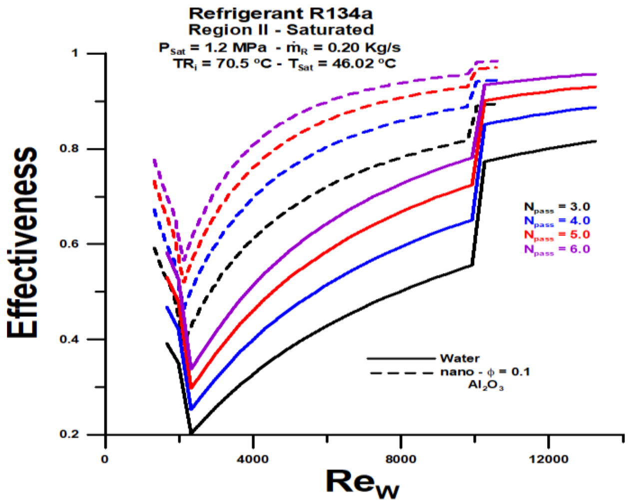

Figure 10 – Influence of the number of passes on the tube on the thermal effectiveness in Region II

4.3 Region III – subcooled liquid

In the region of subcooled liquid of the heat exchanger in question, Region III, already described and represented through Figure 1, three well-defined temperatures are outlet and inlet temperatures in the pipes and inlet temperature refrigerant. The inlet temperature in the pipes is equal to 25.0 °C, and the inlet temperature of the refrigerant is equal to 46.0 °C.

The refrigerant's outlet temperature in Region III is unknown, determined using the methodology described above.

The refrigerant's outlet temperature in Region III, depending on the fluid flow in the tubes, depends on the number of passes in the tube, as represented by Figure 11, for refrigerant flow equal to 0.20 kg/s. The refrigerant outlet temperature is lower, close to 37 ºC, for water flow equal to 0.40 kg/s and the number of passes in the tubes equal to 3. The refrigerant outlet temperature is slightly higher for nanofluids' mass flow rate in the tubes, in all flow rates analyzed. Note that the flow laminarization process, as a function of the fraction of aluminum oxide nanoparticles (Al_2O_3), is observable.

The energy to be absorbed by the refrigerant is defined by the inlet and outlet temperatures and the mass flow rate of the fluid in the tubes. The temperature difference in the refrigerant between the inlet and the outlet is a function of the fluid's thermal capacity in the tubes and the heat exchange area. The fluid with the most significant thermal capacity donates the greatest amount of energy, which allows for a more significant temperature difference for the refrigerant, as represented by Figure 12.

When analyzing the heat exchange as a function of the exchange area, depending on the number of passes in the tube, in Region III, it becomes necessary also to consider the overall heat transfer coefficient.

The global heat transfer coefficient is greater for fewer passes in the tube, as shown in Figure 13. It is evident that the smaller number of passes, that is, the smaller heat exchange area, has a greater influence on the global coefficient heat exchange than the most significant temperature difference between inlet and outlet for the refrigerant. Remembering that the available energy is practically the same (Figure 7), depending on the fluid's temperature entering and leaving the tubes.

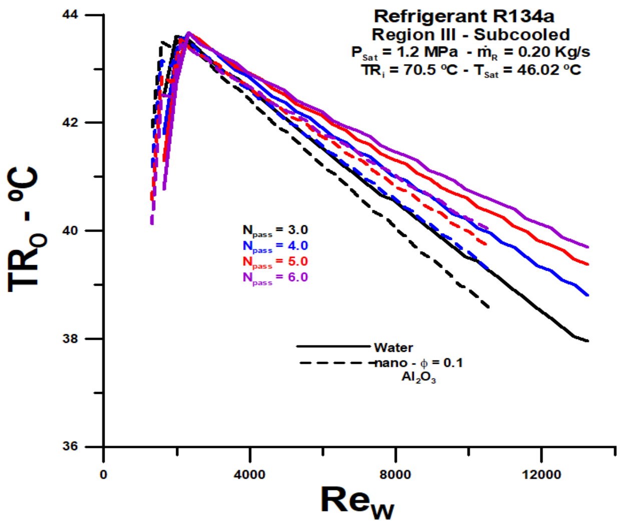

Figure 11 - Influence of the number of passes through the tube on the refrigerant outlet temperature in Region III

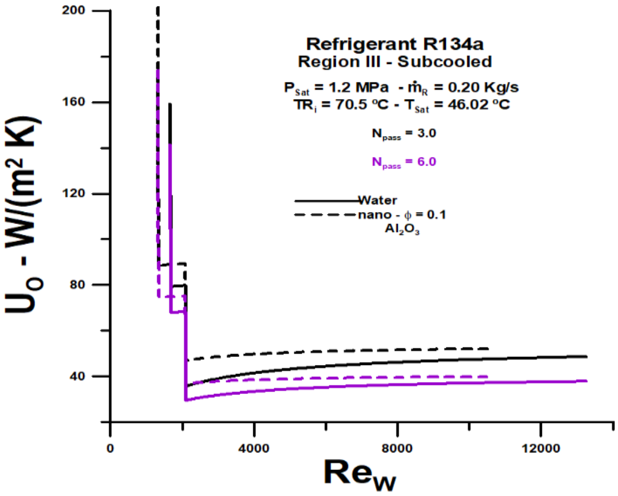

Figure 13 - Global heat transfer coefficient in Region III as a function of the number of passes in the pipe

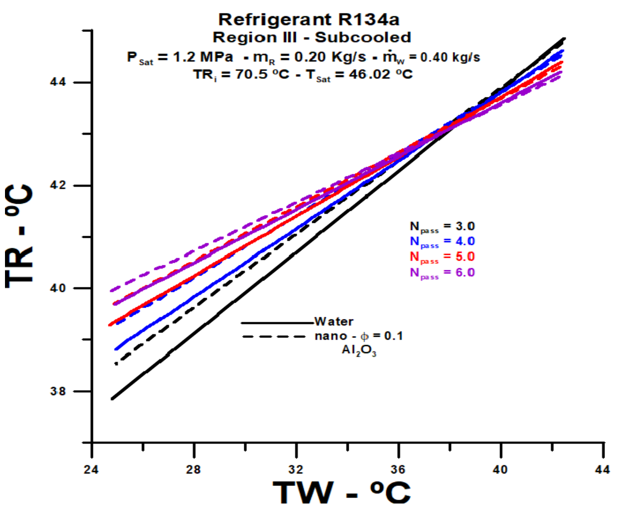

Figure 12 – Influence of the number of passes in the pipe on the temperature of the refrigerant in Region III

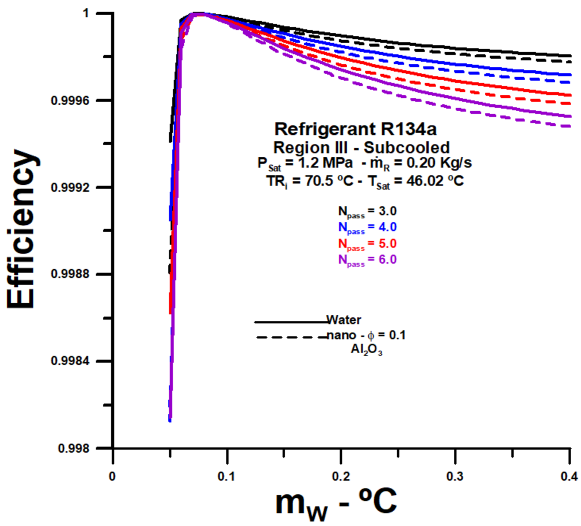

Figure 14 - Influence of the number of passes on the tube on thermal efficiency in Region III

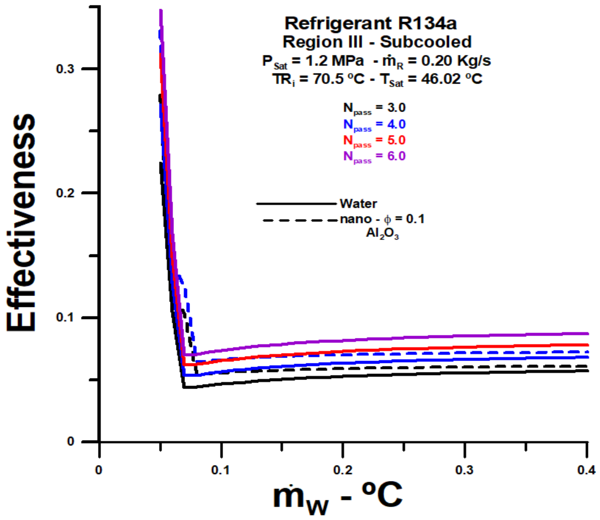

Figure 15 – Influence of the number of passes on the tube on thermal effectiveness in Region III

The thermal efficiency in Region III is exceptionally high, as shown in Figure 14, for the entire range of mass flow and the number of passes in the tube.

The effectiveness is extremely low in Region III, as shown in Figure 15, for the entire range of mass flow in the tube and the number of passes in the tube. It can be observed, in this case, that the effectiveness is slightly higher for a more significant number of passes in the tube and, also, for greater mass flow rates of the fluid in the tube. The heat exchange is shallow, and there is ample scope for increasing effectiveness. However, the fluid inlet temperature in the tube is fixed, equal to 25 °C, and is the limiting factor for greater heat exchange. There are two possibilities to increase the effectiveness in Region III: 1 - decrease the fluid's temperature entering the tube; 2 - increase the refrigerant inlet pressure, increasing the saturation temperature of the refrigerant, thus increasing the temperature difference between fluid outlet and inlet in the tubes.

5 Conclusions

The mass flow rate allows the highest outlet temperature in superheated steam is the lowest possible, equal to 0.05 kg/s.

There is scope for increasing thermal effectiveness in superheated steam. It can be improved with a more significant number of passes in the tube or a change in the inlet temperature of the refrigerant.

The highest inlet temperature for the fluid in the pipe, in the saturated region, is obtained for the lowest flow and the lowest number of passes.

Efficiency in the saturated steam region is 1.0 for a lower flow rate, regardless of the number of passes in the pipe.

The saturated steam region's effectiveness is low for lower flows, rising to values close to 0.8 for a higher flow rate.

The saturated steam region process is efficient for lower mass flow rates of the fluid in the tube but is not effective. However, is highly effective for high mass flow rates.

The thermal efficiency in the subcooled region is exceptionally high for the entire mass flow rate range and passes in the pipe.

The effectiveness is extremely low in the subcooled region for the entire range of mass flow in the tube and the number of passes in the tube.

The subcooled region's effectiveness is slightly higher for a more significant number of passes in the tube and, also, for greater mass flow rates of the fluid in the tube. The heat exchange is shallow, and there is ample scope for increasing effectiveness. The fluid inlet temperature in the pipe equal to 25 °C is one of the limiting factors for greater heat exchange.

Thus, to increase the subcooled region's effectiveness, it is necessary to decrease the fluid's temperature entering the pipe or increase the refrigerant inlet pressure.

References

1. Lee, T.-S., and Mai, J.-W. (2011). Modeling and Simulation of the Heat Transfer Behavior of a Shell-and-Tube Condenser for a Moderately High-Temperature Heat Pump. *In: Ahsan, A., Ed., Two-Phase Flow, Phase Change and Numerical Modeling, InTech, Department of Energy and Refrigerating Air-Conditioning Engineering*, National Taipei University of Technology, Chinese Taipei.
2. Nogueira, E. (2020). Theoretical Analysis of a Shell and Tubes Condenser with R134a Working Refrigerant and Water-Based Oxide of Aluminum Nanofluid (Al_2O_3). *Journal of Materials Science and Chemical Engineering*, Vol. 8, pp. 1–22, https://doi.org/10.4236/msce.2020.811001.
3. Bejan, A. (1987). The Thermodynamic Design of Heat and Mass Transfer Processes and Devices. *Heat and Fluid Flow*, Vol. 8, pp. 258–276, https://doi.org/10.1016/0142-727X(87)90062-2.
4. Fakheri, A. (2007). Heat Exchanger Efficiency. *Transactions of the ASME*, Vol. 129, pp. 1268–1276. https://doi.org/10.1115/1.2739620.
5. Tiwari, R., Maheshwari, G. (2017). Effectiveness and Efficiency Analysis of Parallel Flow and Counter Flow Heat Exchangers. *IJAIEM*, Vol. 6, pp. 314–319.
6. Hermes, C.J. L. (2012). Thermodynamic Design of Condensers and Evaporators: Formulation and Applications. *International Refrigeration and Air Conditioning Conference at Purdue*, July 16–19, pp. 1–9.
7. Nogueira, E. (2020) Thermal Performance in Heat Exchangers by the Irreversibility, Effectiveness, and Efficiency Concepts Using Nanofluids. Journal of Engineering Sciences, 7, F1-F7.

8. Nogueira, E. (2020). Efficiency and Effectiveness Concepts Applied in Shell and Tube Heat Exchanger Using Ethylene Glycol-Water Based Fluid in the Shell with Nanoparticles of Copper Oxide (CuO). *Journal of Materials Science and Chemical Engineering*, Vol. 8, pp. 1–12, https//doi.org/10.4236/msce.2020.88001.
9. Dalkilic, A. S., Wongwises, S. (2011). *Two-Phase Heat Transfer Coefficients of R134a Condensation in Vertical Downward Flow at High Mass Flux, Heat Transfer - Theoretical Analysis, Experimental Investigations, and Industrial Systems*. In: Prof. Aziz Belmiloudi (Ed.), ISBN: 978-953-307-226-5, InTech, Available from: http://www.intechopen.com/books/heat-transfer-theoretical-analysis-experimental-investigations-and-industrialsystems/two-phase-heat-transfer-coefficients-of-r134a-condensation-in-vertical-downward-flow-at-high-mass-fl.
10. Roy, R., and Mandal, B.K. (2014). Computer-Based Thermodynamic Properties of Alternative Refrigerant R-134a. Engineering Sciences International Research Journal, Vol. 2, pp. 163–169.
11. Wen, J., Gu, X., Wang, S., Li, Y., Tu, J. (2017). Numerical investigation on condensation heat transfer and pressure drop characteristics of R134a in horizontal flattened tubes. *International Journal of Refrigeration*, https://doi.org/doi:10.1016/j.ijrefrig.2017.10.024.
12. Kaew-On, J., Naphattharanun, N., Binmud, R., Wongwises, S. (2016). Condensation heat transfer characteristics of R134a flowing inside mini circular and flattened tubes. *International Journal of Heat and Mass Transfer*, Vol. 102, pp. 86–97, http://dx.doi.org/10.1016/j.ijheatmasstransfer.2016.05.095.
13. Albadr, J., Tayal, S., Alasadi, M. (2013). Heat transfer through heat exchanger using Al_2O_3 nanofluid at different concentrations. *Case Studies in Thermal Engineering*, Vol. 1(1), pp. 38–44, http://dx.doi.org/10.1016/j.csite.2013.08.004.
14. Almurtaji, S., Ali, N., Teixeira, J. A., Addali, A. (2020). On the Role of Nanofluids in Thermal-Hydraulic Performance of Heat Exchangers – A Review. *Nanomaterials*, Vol. 10, pp. 2–43, https://doi.org/10.3390/nano10040734.